UNIVERSITY OF BATH

University of Bath

An Equivalent Model of Gas Networks for Dynamic Analysis of Gas-Electricity Systems

Yongzhi Zhou, Chenghong Gu, *Member, IEEE*, Hao Wu, *Member, IEEE*, and Yonghua Song, *Fellow, IEEE*

Abstract— **The increasing coupling between natural gas and electricity systems by gas-fired generation units brings new challenges to system analysis, such as pressure variations due to consumption perturbations of generation units. The emerging issues require revolutionary modeling and analysis techniques.**

This paper proposes a novel model to quantify gas pressure variations due to gas-fired power unit ramping and the impact of constraints from natural gas pressure change on ramp rates of gas-fired plants. By utilizing Laplace transform to resolve the governing equations of gas networks, the proposed model can significantly reduce modeling complexity and computational burden. The dynamic behaviors in time scale in s-domain and spatial partial differential equations are transformed into finite difference equations. By introducing the concept of transfer matrices, the relation between states at each node of gas systems can be expressed by transfer parameter matrices. Additionally, a simplified model is introduced to simply the analysis. The explicit expressions of nodal pressure variations in response to demand change are very convenient for analyzing system dynamic performance under disturbances, identifying the most influential factors. The new models are extensively demonstrated on three natural gas networks and benchmarked with traditional simulation approaches. Results illustrate that they produce very close results with the simulation approach, particularly when gas pipelines are long and enter steady states.

Index Terms—**Natural Gas Network, Electricity Networks, Transfer Matrix, Integrated Energy System, Dynamic Modelling**

I. INTRODUCTION

NATURAL gas and electricity networks are being tightly linked by more gas-fired turbines installed, which can provide fast electricity balancing and relatively clean energy. For example, the current installed capacity of gas power plants in the UK is around 33GW, out of its 75.3 GW total capacity [1]. Thus, the reliable operation of power systems depends not only on the status of electric facilities but also on natural gas infrastructures. On the other hand, the operation of gas-fired power plants also has direct impact natural gas systems. Paper [2] reviews the interdependence of many critical infrastructures,

characterizes the interdependence, and discusses the pros and cons and challenges in integrated analysis. The tight couplings between natural gas and electricity infrastructures need new models and techniques to analyse the underlying impact.

Previous work has devoted a large amount of efforts to analyzing the interactions of natural gas and electricity systems in unit commitment [3-5], risk assessment [6, 7], etc. In [3], both systems are represented as networks, consisting of nodes and arcs with capacity and efficiency constraints considered. Then, the economic efficiency of energy flows in the integrated energy system is evaluated. In [4], an integrated model considering natural gas networks and hydroelectric power plant reservoirs is developed for operational planning of electricity systems. In [6], an integrated model for assessing the impact of the interdependence of electricity and gas networks on electricity system security is proposed. However, linear natural gas network constraints are adopted without considering the nonlinear relationship between gas flow and pressures. Paper [8] reviews the hybrid gas-electricity models and presents a new model to illustrate a few of potential coupling effects between gas and electric power systems. Work in [9] analyzes the impact of natural gas infrastructure contingencies on the operation of electric power systems. These studies mainly use steady state models, where the dynamic behaviors of natural gas networks are neglected. Paper [10] shows that the use of steady-state natural gas flow models may result in impractical results, neglecting the linepack and slower traveling speed of natural gas flows.

Thus, it is essential to develop dynamic models of natural gas networks for integrated gas-electricity system analysis in order to capture their interactions more precisely. Typically, the dynamic behaviors of isothermal gas flow are modeled as continuity and momentum equations [11, 12] with constant temperature. Many numerical methods have been introduced to study the dynamics, such as explicit finite-difference methods, implicit finite-difference methods, and finite element methods [13]. The implicit methods have been widely used because of high accuracy, efficiency and stability [14, 15]. In [10], transient flows modeled as partial differential equations (PDEs), are discretized in space and time, which can result in very large-scale algebraic equations. In [16], a surrogate network flow is used to model the dynamics, which is derived by a model reduction technique proposed in [17]. The pressure fluctuations caused by stochastic gas consumption are modeled in [18], where *diffusive jitter* is used to represent this effect. In [19], the dynamic interactions between a microgrid and

Y. Zhou, H. Wu and Y. Song are with College of Electrical Engineering, Zhejiang University, Hangzhou, 310027, China (email: zhouyongzhi@zju.edu.cn, zjuwuhao@zju.edu.cn, and yhsongcn@zju.edu.cn).

C. Gu is with the Dept. Electronic and Electrical Engineering, University of Bath, Bath, BA2 7AY, UK (email: c.gu@bath.ac.uk). Y. Zhou is now a Visiting Research Scholar at the University of Bath.

small-scale natural gas system are simulated on MATLAB. In the paper, the dynamic behaviors of natural gas in pipes are described by partial differential equations.

The difficulties to characterize gas network dynamics present great challenges for integrated energy system modeling. Simulation approaches are not very convenient to use due to high complexity and not non-analytical features. In addition, they are very time consuming, particularly for large-scale systems. Lastly, some embedded implications of system performance can hardly be obtained by simulation approaches. Thus, it is essential to develop a dynamic model for gas networks which can be easily utilized for integrated gas-electricity system study.

Laplace transform is a common tool to analyze system dynamic behaviors [20, 21]. In paper [20], the equivalent model based on distributed parameters is conducted from a predefined model with known parameters. The model is conducted based on the physical phenomenon of gas systems. Parameters are determined by the characteristics of gas composition and flows with many assumptions on length and diameters, probably compromising accuracy under specified frequencies. Additionally, the work treats a pipe as a whole and intersections are not considered and results are presented in time-delay model. In this paper, Laplace transform is also an essential step for deriving transfer functions and obtaining the relationship between two ends of pipelines. The model is based on transfer functions and numerical formulations, derived from the governing equations of pipelines.

This paper proposes an equivalent model of natural gas networks for dynamic analysis, quantifying gas network pressure variations due to the ramp of gas-fired power plants. The dynamic behaviors in time scale are described in L-domain. By using Laplace transform, discretization spatial partial differential equations (PDEs) are transformed into finite difference equations. By using transfer matrix concept from electrical circuit theory, the relations between state variables can be expressed by transfer matrices. The explicit expression of pressure variations is very convenient for analyzing system performance under disturbance. This paper also examines the impact of constraints from natural gas pressure change on ramp rates of gas-fired plants. The new models are extensively demonstrated on three gas networks and benchmarked with a traditional simulation approach to illustrate the accuracy. Results illustrate that they produce very close results with the simulation approach, particularly when pipelines are long and in steady states. The new models are very useful for analyzing the dynamic couplings of gas-electricity networks, particularly considering the scale of both systems grows dramatically.

The main contribution is summarized as follows: i) the transfer matrix concept in electric circuits is introduced to model pipelines as a cascade of two-port sections, which can easily illustrate the relation between their inputs and outputs; ii) the equivalent model can improve dynamic analysis efficiency for integrated energy systems as the numerical efforts for modeling dynamic behaviors of whole gas systems can be significantly reduced.

The remainder of the paper is organized as follows: Section II introduces the dynamic models of gas networks. Sections III and IV propose full transfer matrix for pipelines and simply the matrix. In Section V, the ramp of gas-fired plants is modelled that bridges gas and electricity networks. Case studies are given in Section VI and Section VII concludes the paper.

II. DYNAMIC GAS FLOW MODEL

This section briefly introduces the dynamic gas flow model and the application of Laplace transform, followed by numerical formulation for the model.

A. Original Gas Pipeline Model

In the dynamic modelling of gas pipelines in short time period, temperature variations and pipe inclination can be neglected, as they slightly change. For a pipeline with the length of L, gas flow model is governed by a series of PDEs on spatial dimension $x \in [0, L]$ and time dimension t [11, 22]

The continuity equation is

$$\partial_t \pi + \frac{c^2}{A} \partial_x \dot{m} = 0 \tag{1}$$

where, π is pressure (Pa), $\dot{m}$ is mass flow (kg/s), and A is the cross section area of the pipeline (m²). Here, c is sound speed, which is decided by

$$c = \sqrt{ZRT} \tag{2}$$

where, Z is compressibility factor, R is gas constant and T is temperature.

The momentum equation is

$$\partial_t \dot{m} + \frac{c^2}{A} \partial_x \left(\frac{\dot{m}^2}{\pi} \right) + A \cdot \partial_x \pi + \frac{fc^2 \dot{m} |\dot{m}|}{2DA\pi} = 0 \tag{3}$$

where, D is the diameter of the pipeline, f is friction factor

Because gas flow velocities are normally small compared to sound speed, gas inertia term $\partial_t \dot{m}$ and convective inertia term $\partial_x (\dot{m}^2/\pi)$ in (3) are neglected [14, 18]. Only friction losses term $\partial_x \pi$ is considered in the momentum equation.

The solutions to the dynamic model in (1)-(3) on $t \in [0, \tau]$ and $x \in [0, L]$ require the initial and boundary conditions

$$\forall x \in [0, L]: \quad \dot{m}(0; x) = \dot{m}_0(x), \tag{4}$$

$$\forall t \in [0, \tau]: \quad \dot{m}(t; 0) = \dot{m}_{in}(t), \dot{m}(t; L) = \dot{m}_{out}(t). \tag{5}$$

$$\pi(0; 0) = \pi_0 \tag{6}$$

where, $\dot{m}_0$ is initial mass flow in the pipeline, $\dot{m}_{in}$ and $\dot{m}_{out}$ are injections at the inlet and outlet, and π_0 is the initial pressure at the beginning of the pipeline.

As discussed, traditional simulation-based approaches for resolving the models are not only time consuming but also complex. In linear dynamic systems, *Laplace Transform* [23] can transform differential equations into polynomial algebraic equations, i.e. from the time domain to frequency domain so

that dynamic analysis can be simplified.

B. Linearization and Laplace Transform

In order to simplify the analysis and apply *Laplace Transform* here, the nonlinear gas flow model is linearized around a steady operation point in uniform mass flow along pipelines. It is assumed that gas flow directions do not change when gas demand fluctuates, and thus $\dot{m}|\dot{m}| = \dot{m}^2$. Then, (1) and (3) are linearized as

$$\partial_t \Delta\pi(t;x) + \frac{c^2}{A}\partial_x \Delta\dot{m}(t;x) = 0 \qquad (7)$$

$$A\cdot\partial_x \Delta\pi(t;x) + \frac{fc^2\dot{m}_{st}}{DA\pi_{st}}\Delta\dot{m}(t;x) - \frac{fc^2\dot{m}_{st}^2}{2DA\pi_{st}^2}\Delta\pi(t;x) = 0 \quad (8)$$

where, π_{st} is average steady pressure and $\dot{m}_{st}$ is steady mass flow at the operation point.

Here, *Laplace Transform* is applied to the time differential terms in (7) and (8) so that the model is transformed from time domain into *L*-domain. Then, the dynamic gas flow equations only have spatial differential terms

$$s\cdot\Delta\Pi(s;x) + \frac{c^2}{A}\partial_x \Delta\dot{M}(s;x) = 0 \qquad (9)$$

$$A\cdot\partial_x \Delta\Pi(s;x) + \frac{fc^2\dot{m}_{st}}{DA\pi_{st}}\Delta\dot{M}(s;x) - \frac{fc^2\dot{m}_{st}^2}{2DA\pi_{st}^2}\Delta\Pi(s;x) = 0 \quad (10)$$

where, $\Delta\Pi$ and $\Delta\dot{M}$ are the pressure and mass flow of the gas pipeline on *L*-domain.

C. Numerical Formulation

The governing PDEs in (9) and (10) are discretized into algebraic equations on *s*-domain and space so that they can be resolved by implicit finite difference methods.
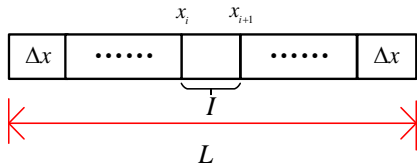

Fig. 1. A piecewise natural gas pipeline.

As shown in Fig. 1, a pipeline with the length of *L* is divided into *N* sections. For section *I* between points x_i and x_{i+1}, the spatial derivatives can be approximated by

$$\frac{\partial Y(s;x_I)}{\partial x} = \frac{Y(s;x_{i+1}) - Y(s;x_i)}{\Delta x} + o(\Delta x^2) \qquad (11)$$

where, the term *Y* representing states π and $\dot{m}$, decided by

$$Y(s;x_I) = \frac{Y(s;x_{i+1}) + Y(s;x_i)}{2} + o(\Delta x^2) \qquad (12)$$

It should be noted that this method is second-order accurate [22]. By discretizing (9) and (10) with (11), the governing equations are transformed into (13) and (14) with $1 \le i \le N$

$$s\cdot\frac{\Delta\Pi(s;x_{i+1}) + \Delta\Pi(s;x_i)}{2} + \frac{A}{c^2}\frac{\Delta\dot{M}(s;x_{i+1}) - \Delta\dot{M}(s;x_i)}{\Delta x} = 0 \qquad (13)$$

$$A\frac{\Delta\Pi(s;x_{i+1}) - \Delta\Pi(s;x_i)}{\Delta x} + \frac{fc^2\dot{m}_{st}}{DA\pi_{st}}\frac{\Delta\dot{M}(s;x_{i+1}) + \Delta\dot{M}(s;x_i)}{2}$$
$$- \frac{fc^2\dot{m}_{st}^2}{2DA\pi_{st}^2}\frac{\Delta\Pi(s;x_{i+1}) + \Delta\Pi(s;x_i)}{2} = 0 \qquad (14)$$

For a pipeline with $N+1$ points, i.e. N sections, there are $2N$ equations and $2N+2$ unknown variables in (13) and (14). To ensure the solvability, two additional equations are needed, which are constructed based on the boundary conditions: i) the pressure setting at the inlet of the pipeline, and ii) the mass flow demand at the outlet of the pipeline. Thus, the number of equations is equal to the number of unknown variables, indicating that the equations can be mathematically solved.

III. TRANSFER MATRIX OF GAS PIPELINES

In the dynamic analysis of a gas pipeline, only the states of pressure and mass flow at the inlet and outlet are concerned. It is similar to a two-port network in electrical engineering, where the relation between voltages and currents at input and output ends are to be determined. Thus, in this section, the concept of transfer matrix for a two-port network is extended to represent the states of a gas pipeline at its both ends.

A. Transfer Matrix for a Two-port Network

In electrical engineering, a two-port network is used to represent isolated portions of a large/long circuit. The inner properties are regarded as a black box, represented by a matrix, named *transfer matrix*. This simplification makes analysis very easy, without detailed modeling of internal states.

Fig. 2. A two-port network.

Fig. 2 is a section of an electric circuit with two state variables at each end. It can be represented by a transfer matrix

$$\begin{pmatrix} a_2 \\ b_2 \end{pmatrix} = \begin{pmatrix} T_{11} & T_{12} \\ T_{21} & T_{22} \end{pmatrix}\begin{pmatrix} a_1 \\ b_1 \end{pmatrix} \qquad (15)$$

where, a_1, a_2, b_1, b_2 are state variables, and T_{11}, T_{12}, T_{21}, and T_{22} are the elements of the transfer matrix, decided by the physical characteristics of the section.

The output of one cascade section of a long circuit on the left side is the input for the next cascade section on the right side. Thus, the transfer matrix can be easily extended to represent a network of a series of cascade two-port sections, linked from left to right. Hence, the transfer matrix of *N* cascade two-port sections with identical physical features is

$$\begin{pmatrix} a_{N+1} \\ b_{N+1} \end{pmatrix} = \underbrace{\begin{pmatrix} T_{11} & T_{12} \\ T_{21} & T_{22} \end{pmatrix}\cdots\begin{pmatrix} T_{11} & T_{12} \\ T_{21} & T_{22} \end{pmatrix}}_{N}\begin{pmatrix} a_1 \\ b_1 \end{pmatrix} \qquad (16)$$

where, a_{N+1} and b_{N+1} are the output state variables at the end of the series of two-port sections.

B. Transfer Matrix for a Single Pipeline

In this paper, the transfer matrix is used to represent the relation between state variables, i.e. pressure and mass flow, at the inlet and outlet of a gas pipeline.

$$\Delta\pi(x_i) \qquad \Delta\pi(x_{i+1})$$
$$\boxed{\Delta x}$$
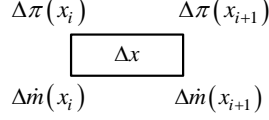$$\Delta\dot{m}(x_i) \qquad \Delta\dot{m}(x_{i+1})$$

Fig. 3. A representative pipeline section.

For a section pipeline shown in Fig. 3, there are two states on each side, pressure and gas flow. Similarly to the quadripole in an electrical circuit, it can be modeled as a two-port network, whose transfer relation is

$$\begin{pmatrix} \Delta\Pi(x_{i+1}) \\ \Delta\dot{M}(x_{i+1}) \end{pmatrix} = \mathbf{T}(s)\begin{pmatrix} \Delta\Pi(x_i) \\ \Delta\dot{M}(x_i) \end{pmatrix} = \begin{pmatrix} T_{11} & T_{12} \\ T_{21} & T_{22} \end{pmatrix}\begin{pmatrix} \Delta\Pi(x_i) \\ \Delta\dot{M}(x_i) \end{pmatrix} \quad (17)$$

where, $\mathbf{T}(s)$ is the transfer matrix determined by (13) and (14) and the specific elements are

$$\begin{cases} T_{11} = -\left(s \cdot A f \dot{m}_{st} \pi_{st} \Delta x^2 + 4A^2 D\pi_{st}^2 + fc^2\dot{m}_{st}^2\Delta x\right)/T_{cmn} \\ T_{12} = \left(4fc^2\dot{m}_{st}\pi_{st}\Delta x\right)/T_{cmn} \\ T_{21} = \left(s \cdot 4A^3 D\pi_{st}^2\Delta x\right)/\left(c^2 T_{cmn}\right) \\ T_{22} = \left(-s \cdot A f \dot{m}_{st}\pi_{st}\Delta x^2 - 4A^2 D\pi_{st}^2 + fc^2\dot{m}_{st}^2\Delta x\right)/T_{cmn} \end{cases} \quad (18)$$

where, $T_{cmn} = s \cdot A f \dot{m}_{st}\pi_{st}\Delta x^2 - 4A^2 D\pi_{st}^2 + fc^2\dot{m}_{st}^2\Delta x$.

The transfer matrix relates the state variables at left-hand side port to the state variables at right-hand side port. The relation between the two groups of variables are

$$\begin{pmatrix} \Delta\Pi(x_{N+1}) \\ \Delta\dot{M}(x_{N+1}) \end{pmatrix} = \mathbf{T}^N\begin{pmatrix} \Delta\Pi(x_1) \\ \Delta\dot{M}(x_1) \end{pmatrix} = \begin{pmatrix} T_{N11} & T_{N12} \\ T_{N21} & T_{N22} \end{pmatrix}\begin{pmatrix} \Delta\Pi(x_1) \\ \Delta\dot{M}(x_1) \end{pmatrix} \quad (19)$$

If assuming that the pressure at the inlet of the pipeline is constant, then

$$\Delta\Pi(x_1) = 0 \quad (20)$$

When there is a gas demand variation at the end of the pipeline, the pressure fluctuations at pipeline end, $\Delta\Pi(x_{N+1})$, and the mass flow at inlet, $\Delta\dot{M}(x_1)$, can be quantified as

$$\Delta\Pi(x_{N+1}) = \frac{T_{N12}(s)}{T_{N22}(s)} \cdot \Delta\dot{M}(x_{N+1}) \quad (21)$$

$$\Delta\dot{M}(x_1) = \frac{1}{T_{N22}(s)} \cdot \Delta\dot{M}(x_{N+1}) \quad (22)$$

When the number of sections is large, the order of transfer functions' denominators in (21) and (22) could be high, making analysis difficult. Thus, an approach to simplify the transfer matrix is required, which will be discussed in Section IV.

C. Transfer Matrix for a Meshed Gas Network

Here, the transfer matrix for a single pipeline is extended to a meshed gas network. It is assumed that the directions of gas flows in pipelines remain unchanged when gas demand fluctuates at any specific sites.

In a network with N_b branches and N_n nodes, the transfer matrix for the pipeline from node i to j is

$$\begin{pmatrix} \Delta\Pi_j \\ \Delta\dot{M}_j \end{pmatrix} = \mathbf{T}_{i\to j}\begin{pmatrix} \Delta\Pi_i \\ \Delta\dot{M}_i \end{pmatrix} \quad (23)$$

where, $\Delta\dot{M}_i$ and $\Delta\dot{M}_j$ are the mass flow in the pipeline at node i and node j, $\mathbf{T}_{i\to j}$ is the transfer matrix of this single pipeline constructed in subsection III-B, and the subscript $i \to j$ means that the gas flows from node i to j.

According to the law of mass conservation, the mass flow at node i should meet

$$\sum_{B_{i\to j}}\Delta\dot{M}_i - \sum_{B_{j\to i}}\Delta\dot{M}_i + \Delta\dot{M}_i^{load} - \Delta\dot{M}_i^{inject} = 0 \quad (24)$$

where, $B_{i\to j}$ and $B_{j\to i}$ are the branch sets related to node i, $\sum_{B_{i\to j}}\Delta\dot{M}_i$ denotes the total gas flow leaving node-i, $\sum_{B_{j\to i}}\Delta\dot{M}_i$ denotes the total gas flow entering node-i, $\Delta\dot{M}_i^{load}$ is gas demand at node i, and $\Delta\dot{M}_i^{inject}$ is gas injection at node i.

As (23) and (24) are linear equations, the relationship between any two state variables can be obtained by eliminating other variables.

D. Simplification of the Transfer Function

In order to simplify analysis, high-order elements in the transfer function models in (19)-(22) are approximated with a lower-order model, which can inherit the dynamic and steady-state characteristics.

In inverse Laplace transform, it is known that a small time constant leads to fast dynamics. The dynamics of natural gas systems are usually very slow compared to electricity networks, and thus it is reasonable to approximate high-frequency dynamics by using approximate equivalent terms. If a transfer function $T(s)$ has a denominator of the r-th order polynomial, the normalized step response for $T(s)$ can be represented as

$$\frac{T(s)}{s} = \frac{m_0}{s} + \frac{m_1}{(\tau_1 s + 1)} + \cdots + \frac{m_r}{(\tau_r s + 1)} \quad (25)$$

where, $\tau_1 > \cdots > \tau_r$ and they are denominator time constants, and $m_0, \cdots, m_r$ are gain coefficients.

To derive the approximation, for a small value of s, the following feature of transfer functions is considered [24]

$$\frac{1}{1+\tau s} \approx 1 - \tau s \qquad (26)$$

Then, for the terms in (25) whose denominator time constants are less than τ_{set} (the minimum threshold time constant considered), the following relation holds

$$\sum_{\tau_i \leq \tau_{set}} \frac{m_i}{(\tau_i s + 1)} \approx \sum_{\tau_i \leq \tau_{set}} (m_i - m_i \tau_i s)$$

$$\approx \sum_{\tau_i \leq \tau_{set}} m_i \left/ \left(1 + s \frac{\displaystyle\sum_{\tau_i \leq \tau_{set}} m_i \tau_i}{\displaystyle\sum_{\tau_i \leq \tau_{set}} m_i} \right) \right. \qquad (27)$$

where, the second approximation is a lag dominant process, representing the terms with fast dynamics.

By approximating the terms with small time constants, the transfer functions can be expressed in a simplified form but the dynamic characteristics are still preserved.

IV. IMPLEMENTATION STEPS AND ERROR ANALYSIS

This subsection provides the implementation steps of the proposed approach and discusses potential errors.

A. Implementation Steps

The proposed model can be easily implemented through the following steps for dynamic study:

Step 1) use natural gas system data to build dynamic models, which are continuity equation in (1) and momentum equation in (3);

Step 2) Linearize the governing equations of (1) and (3), where the resultant equations are in (7) and (8);

Step 3) Use Laplace transform to convert (7) and (8) from time domain into frequency domain in (9) and (10);

Step 4) Discretize (9) and (10) into algebraic equations on s-domain and space in (13) and (14) so that they can be resolved by implicit finite difference methods;

Step 5) Use transfer matrix concept to relate input state variables and output variables in (17)-(19) for a single pipeline;

Step 6) Combine (23) and (24) for meshed natural gas networks to study the relation of inputs and outputs;

Step 7) Use (27) to simplify the relation in (24).

B. Error Analysis

It is noted that errors may appear in each step:

1) *Linearization:* In the first step, the linearization of original pipelines will inevitably cause errors because of neglected nonlinearity. The level of errors is very much decided by the nonlinearity of the original model. If the model has a high level of nonlinearity, the error from our proposed model could be large, vice versa.

2) *Discretization:* In solving dynamic systems governed by partial differential equations, the most common way is to transfer the equations into finite difference equations. In this step, errors are related to the number of discretization and

measures of numerical simulation. The errors can be reduced if bigger discretization numbers are used.

3) *Laplace Transformation:* Once the models are linearized, Laplace transform has no influence on the accuracy.

4) *Transfer Matrix:* Similarly, for linear systems, the transfer matrix can fully capture system characteristics and introduces no errors once the models are linearized.

5) *Simplification:* The full transfer matrix can be transformed into a simplified form by neglecting high-frequency dynamics if they are small, producing errors. In fact, it is hard to prove that the majority of natural gas system dynamics are low frequencies because different pipelines may have distinctive parameters. In the case that all dynamics are desirable, full transfer functions should be utilized.

V. IMPACT OF THE RAMP OF GAS-FIRED POWER PLANTS

Natural gas and electricity systems are coupled by natural gas-fired power plants, which consume gas to generate electricity, particularly for balancing the fluctuation of wind power and electricity demand. In order to illustrate how the proposed model can be used, this paper investigates the impact of: i) gas-fired plants ramp on gas network pressures due to electricity generation fluctuations; and ii) the constraints from gas pressure change limits on ramp rates of gas-fired plants.

A. Model of Gas-fired Plants

If gas-fired plants are used to balance electricity variations, each plant has a ramp rate to assist the system operator in determining the speed of the called plant to respond to impending imbalance. The ramp rates of individual generating units are normally different because of distinct operating characteristics and parameters of plants.

The coupling gas-fired power plants are modeled according to the heat value of natural gas and conversion efficiency. The efficiency of energy conversion is formulated by [25]

$$\Delta P_{gen}^i = HR_i \cdot \eta_i \qquad (28)$$

where, η_i is the coefficients of heat rate and HR is heat value of natural gas.

Then, the gas flow changed for the generation is

$$\Delta \dot{m}_i = \frac{HR_i}{GHV}, \qquad (29)$$

where GHV is gross heat value of natural gas.

B. Change Rates of Gas Pressure

Gas-fired power plants are big consumers of natural gas and their rapid change of consumption will inevitably cause fast gas pressure fluctuation, which may be harmful to other gas-fired equipment. For example, the M701F gas-fired turbine by *Mitsubishi* must be operated with the change rate of gas pressure less than 80 kPa/s, otherwise, it will be tripped. If the ramp rates of gas-fired plants are too large, gas pressure controllers of some equipment may not be able to handle such rapid changes properly. It can be disastrous to other gas consumers without pressure controllers. Therefore, the operation of gas-fired plants should respect the constraints of

gas pressure change rates in order to ensure gas system safety.

VI. CASE STUDIES

In this section, the effectiveness of the proposed models is tested in three cases: i) a single pipeline, and ii) two real gas networks with 6 nodes and 15 nodes.

A. Case I: A Single Pipeline

The parameters of a single pipeline in Figure 4 are given in Table I. The steady state flow is assumed to be 30kg/s. Its beginning is assumed to be pressure control and the gas flow at the end changes caused by a gas-fired power plant. Here, the normalized step response of the pressure at pipeline end is investigated by three models: traditional simulation, full transfer function, and simplified transfer function.
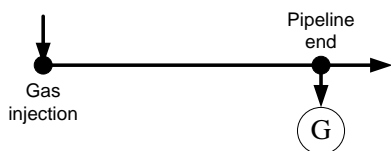
Fig.4. A single pipeline model

TABLE I
PARAMETERS OF THE PIPELINE IN CASE I

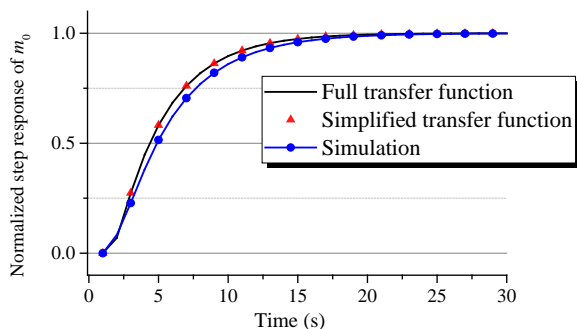| Symbol	Value	Symbol	Value
D	0.6 m	Z	0.9
f	0.05	R	500 J/(kg.K^{-1})
Δx	100 m	T	278 K
π_{st}	4 MPa	$\dot{m}_{st}$	30 kg/s

1) Accuracy

Fig. 5. Normalized step response with 2000 m length pipeline.

Results from the time-step simulation using the original model are used as a benchmark to illustrate the accuracy of the two proposed transfer function models. The simplified transfer function is derived from the full transfer function by approximating high-frequency dynamic elements whose time constants are less than 1 second. Two scenarios of different pipeline length, 2000 meters and 7000 meters, are considered.
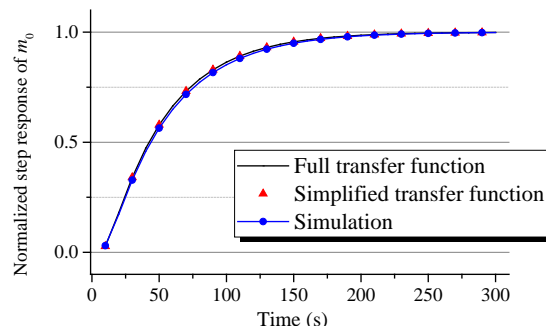
Fig. 6. Normalized step response with 7000 m length pipeline.

In Fig.5, the triangles represent results from the simplified model, the dots are results from the simulation model, and the black line represents results from the full transfer function. Clearly, the results from the proposed equivalent models are very close to simulation results, particularly when elapsed time is longer than 20 seconds, although the difference is relatively big from 5~15 seconds. Compared with simulation results, the average percentage errors from the full and simplified transfer functions are 0.009% and 1.2%, respectively. The results from the simplified transfer function are almost the same with those from the full transfer function. It is because the fast dynamics less than 1 second have little influence.

Fig. 6 compares the results from the three approaches for a longer pipeline of 7000 meters. As seen, the dynamics are much slower compared to those in Fig.5. The average percentage errors of the full and simplified transfer functions are 0.0006% and 0.34% respectively, which are smaller than those in the case of the 2000-meter pipe. In the 2000 meter length case, the pressure at pipeline end needs only about 20 seconds to reach steady state, while in this case, the time is about 3 minutes. It clearly illustrates that the dynamics of long natural pipelines are very slow compared to electric networks.

TABLE II
THE FIRST THREE DENOMINATOR TIME CONSTANTS

Length (km)	τ_1 (s)	τ_2 (s)	τ_3 (s)
5	22.56	2.49	0.57
6	32.53	3.57	1.28
7	44.34	4.87	1.74
8	58.00	6.36	2.28
9	73.53	8.06	2.89
10	90.92	9.96	3.57
20	369.15	39.89	14.29
30	843.15	89.89	32.18
40	1521.69	160.05	57.23

To further investigate pressure response speed at pipeline ends in response to demand perturbations, Table II provides the first three denominator time constants with different pipeline length. As length increases, the time constants become larger, indicating that longer pipelines have slower transient behaviors. When it is 5km, the first-order time constant is 22.56 seconds, which grows exponentially to 1521.69 seconds for the 40km

case. By contrast, the third-order time constants increase fairly slowly, from 0.57 seconds to 57.23 seconds.

Equations (30) and (31) illustrate the unit pressure variations at the end of the pipeline with respect to time when the power plant increases its demand by 10MW.

$$\pi(t) \approx 1 + 0.316e^{-0.141t} - 1.27e^{-0.1724t} \qquad (30)$$

$$\pi(t) \approx 1 + 0.3e^{-0.000562t} - 1.256e^{-0.000657t} \qquad (31)$$

2) Influence of section numbers

This subsection investigates the impact of pipeline cutting numbers on the precision of the proposed models, i.e. PDEs approximated by finite difference equations. A pipeline of 10km is chosen as an example and the results are provided in Fig. 7. All parameters for the pipeline are in Table I and the simulation time is 5 min. The results from numerical simulation are used as a benchmark, where the time step is 10s and section length in the finite implicit method is 500m. For the equivalent model, if only one section is considered, i.e., $N = 1$, the results involve large errors compared to those from the simulation approach, especially at the start of transience. If $N = 2$, the results are much better than those with $N = 1$, but still involve large errors within the first 50 seconds. When $N = 5$, where Δx is 2km, the results are very close to the simulation results along all 300 seconds. It is mainly because that with a small number of discretization, the finite difference equations cannot fully reflect the characteristics of partial differential equations.
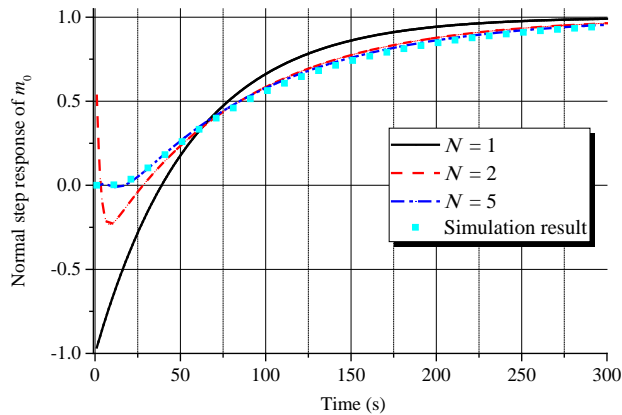

Fig. 7. Normalized step response with different numbers of sections.

3) Influence of steady gas flow

This subsection investigates the properties of natural gas flows under perturbations. Fig.8 provides the results of the largest denominator time constant of a pipeline of 8000 meters under various steady gas flows. Apparently, the time constant is largely in linear relation with steady gas flows. When gas flow is 20kg/s, the largest time constant is around 38 seconds, which grows to around 100 seconds when the gas flow is approximately 50kg/s. It indicates that with larger gas flow, it will take longer for pipeline pressure to enter state states.
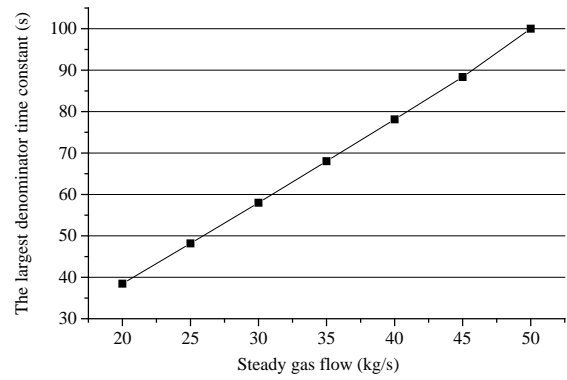

Fig. 8. Relation between steady gas flow and largest dominator time constant.

B. Case II: 6-Node Gas Network

In this subsection, a 6-node gas network adopted from the natural gas system of *The Consumer Power Co.* in the US [26] is used to illustrate the effectiveness of the proposed models. Its configuration is in Fig.9 and the parameters are in Table III.

Node 1 is assumed to be in pressure control mode whose pressure is maintained at 4.0 MPa, and node 2 is in mass flow controlled mode, whose gas injection is constant. Two gas-fired generators denoted as G_1 and G_2, are connected at nodes 4 and 5, whose heat rate is assumed to be 2.89 MJ/MW. The gross heat value of natural gas is 47 MJ/kg [27]. It is assumed that the fluctuations of electricity need to be suppressed by the two gas-fired plants in one minute.
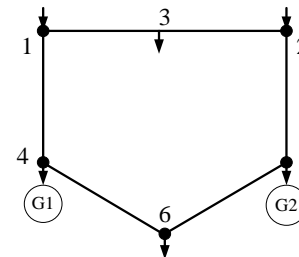

Fig. 9. A 6-node gas network.

TABLE III
PARAMETERS OF 6-NODE GAS NETWORK

			Pipeline parameters			
Branch	From	To	L (km)	f	D (m)	Flow (kg/s)
1	1	3	57.0	0.010	0.50	-4.6
2	1	4	48.6	0.011	0.44	17.6
3	2	3	25.7	0.010	0.50	10.6
4	2	5	26.6	0.013	0.60	34.4
5	4	6	21.4	0.011	0.39	-8.4
6	5	6	36.6	0.013	0.60	26.4

		Node parameters			
Node	2	3	4	5	6
Gas injection (kg/s)	45.0	-6.0	-26.0	-8.0	-18.0
Pressure (MPa)	4.01	4.032	3.738	3.902	3.789

The steady states of all pipelines and nodes are also provided

in Table III, where the state flows are in column 7 and nodal results of gas injection and pressures are at the bottom. The negative gas injection means demand. The pressures at nodes 4 and 6 are the lowest due to large consumption. The second-order transfer functions are employed to approximate the dynamics of each pipeline that is divided into 40 sections.

1) Accuracy comparison with simulation results

Here, we focus on the pressure response at node 5 in response to the output change of G_1 at node 4. Simulation results are used as a benchmark to validate the proposed model, where the time step of simulation is 1 minute.
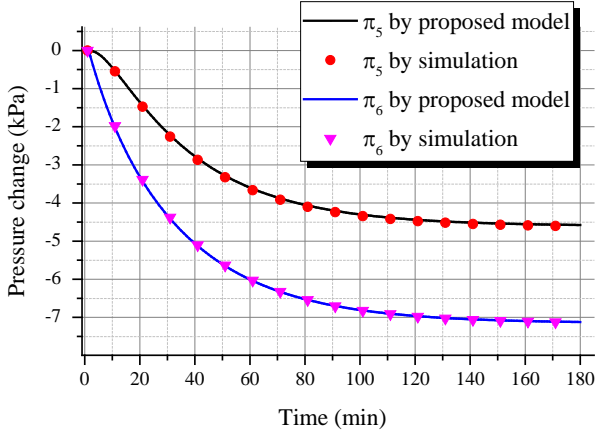

Fig. 10. Normal step (10MW) response of pressure at nodes 5 and 6.

Fig. 10 presents the results by the proposed and simulation methods with 10MW step change of gas demand increase at G_1. It can be seen that the results of the proposed model are very close to those from the simulation for both nodes 5 and 6. The pressures at the two nodes drop by around 4.5kPa and 7kPa respectively compared to original steady state values. The pressure at node 6 drops more sharply than that at node 5, and the biggest difference is around 2.5kPa when the system reaches steady state. It is mainly because that node 5 is further away from node 4 than node 6. Another interesting point is that because the average distance between all nodes is about 36 km, the dynamic response of the system is very slow, roughly taking 2 hours for it to reach steady state.
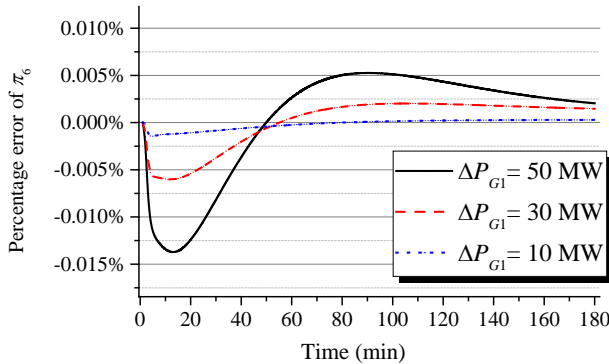

Fig. 11. Pressure percentage error of normal step response at node 6.

To further investigate the precision of the proposed simplified model, Fig. 11 gives the pressure percentage errors

at node 6 under nodal step response when the gas-fired plant at node 4 increases its electricity output. Three scenarios are considered, where the equivalent gas consumption increases at node 4 are 10MW, 30MW and 50MW respectively. Apparently, when the gas demand fluctuates heavily, the errors from the introduced model are larger, particularly when the dynamic starts. However, the errors are very small in amount, within the range of -0.015%~0.005% and drop dramatically with the system entering the steady state.

When G_1 increases its demand by 10 MW equivalent gas, the response of pressure changes at nodes 5 and 6 can be obtained by the simplified model, analytically given in (32) and (33)

$$\Delta\pi_5(t) \approx -4638.7 - 1192e^{-0.0025t} + 5870.63e^{-0.0005t}\ (kPa) \quad (32)$$

$$\Delta\pi_6(t) \approx -7153.67 + 581.4e^{-0.0022t} + 6706.34e^{-0.0005t}\ (kPa) \quad (33)$$

They explicitly illustrate the pressure variations at nodes 5 and 6 with time, very convenient for understating pressure change. This is one key advantage of the proposed models over the traditional simulation approach, which can hardly express pressure variations with analytical equations.

2) Impact of gas pressure change limits on gas-fired plants

Considering the constraints of pressure change rates, the ramp limit of each gas-fired plant can be obtained from the proposed model. Table IV shows the maximum ramp rates under various gas pressure change constraints. Clearly, the ramp limit becomes larger with a bigger tolerance of gas pressure fluctuations. When the pressure change rate is 60 kPa/s, the upper ramp rates of G_1 and G_2 are 15.5 MW/min and 17.1 MW/min, which increase to 20.7 MW/min and 22.8 MW/min when the pressure limit is 80 kPa/s. The results imply that the constraints from gas systems greatly affect the unit commitment of electricity power generation.

TABLE IV
THE RAMP LIMITS OF EACH GAS-FIRED PLANTS

Limit of gas pressure change rate (kPa/s)	G_1 (MW/min)	G_2 (MW/min)
60	15.5	17.1
80	20.7	22.8
100	25.9	28.5
120	31.1	34.2

C. Case III: 15-Node Gas Network

In this subsection, the new model is further demonstrated on a practical 15-node gas network from [26] in Fig. 12. Two gas-fired plants are connected to NG-4 and NG-15.
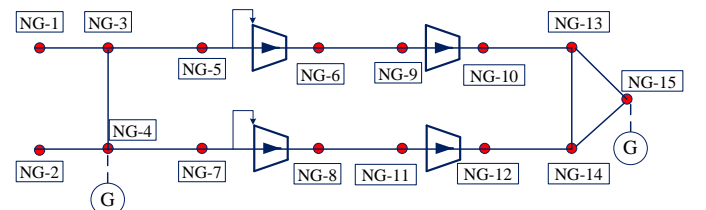

Fig. 12. A 15-node gas network.

With 10MW step change of gas demand increase at NG-15, the responses of gas pressure at NG-4 and NG-15 are

$$\Delta\pi_{NG-4} \approx -80.8 + 5.4e^{-2.2\times10^{-4}t} + 76.21e^{-3.5\times10^{-5}t} \ (kPa) \quad (34)$$

$$\Delta\pi_{NG-15} \approx -526.2 + 15.4e^{-2.2\times10^{-4}t} + 517.7e^{-3.5\times10^{-5}t} \ (kPa) \quad (35)$$
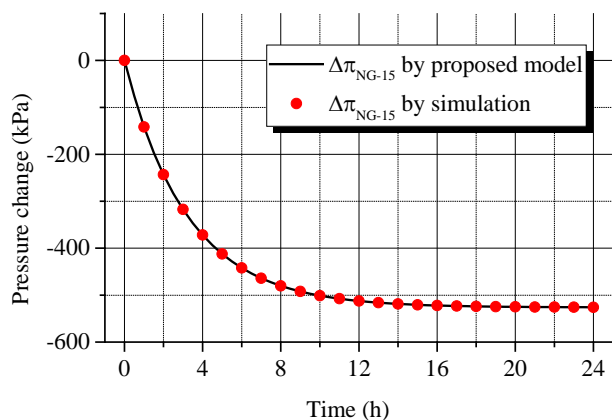

Fig. 13. Normal step (10MW) response of pressure at nodes 5 and 6.

Fig. 13 compares the results of $\Delta\pi_{NG-15}$ from the two methods. It can be seen that the results are very close, which means the proposed method is still effective for large-scale systems. Due to that the total length of all pipelines is over 1600 km, it roughly takes 12 hours for the system to reach steady state. When pipelines are longer, more gas can be stored in pipelines, working as buffers, which can absorb the disturbance. From this point, if we are only concerned with slow dynamics, other simplified models could be derived for example modelling pipelines as gas tanks.

VII. CONCLUSION

This paper proposes a novel method to quantify gas pressure variations due to gas-fired power plant operation and the impact of constraints from natural gas pressure change on ramp rates of gas-fired plants. Through extensive demonstration, the following observations are reached:

- Gas demand variations affect the pressures of other nodes and the degrees are decided by variation size and location. Compared to electricity networks, the dynamics of natural gas systems are very slow and high-frequency dynamics can be neglected in most cases as they have little impact on systems.
- The proposed models can significantly reduce computational burden by utilizing Laplace transform theory to analytically resolve the governing equations of gas networks. Results illustrate that they produce very close results with simulation approaches, particularly when pipelines are long and entering steady states.
- The explicit expressions of pressure variations in response to demand change are very convenient for analyzing system performance under disturbances and identifying the most influential frequency elements.

It is admitted that the designed models also come along with disadvantages, such as:

- The proposed simplified model is derived from linearized

model and thus if the disturbances in natural systems are very large, big errors could appear;
- The model can only respect one-directional gas flows and is not able to handle the case of bi-directional gas flows in pipes;
- There are many compressors and pressure controllers in gas systems, whose dynamics are neglected in the model. The applicability of the models and concept to their dynamics needs further investigation.

Future work will be dedicated to the detailed modelling of gas-fired power plants and other key components of gas systems, such as compressors. The effort will be also paid to investigating the potential to designing models which can represent pipelines with respect to various frequency dynamics.

REFERENCES

[1] DECC. (2015). *Electricity statistics*. Available: https://www.gov.uk/government/collections/electricity-statistics

[2] S. M. Rinaldi, J. P. Peerenboom, and T. K. Kelly, "Identifying, understanding, and analyzing critical infrastructure interdependencies," *Control Systems, IEEE,* vol. 21, pp. 11-25, 2001.

[3] A. Quelhas, E. Gil, J. D. McCalley, and S. M. Ryan, "A multiperiod generalized network flow model of the US integrated energy system: Part I - Model description," *IEEE Transactions on Power Systems,* vol. 22, pp. 829-836, May 2007.

[4] C. R. Cintra, C. L. T. Borges, and D. M. Falcao, "A Simplified Operation Planning Model Considering Natural Gas Network and Reservoir Constraints," *2010 IEE PES Transmission and Distribution Conference and Exposition: Smart Solutions for a Changing World,* 2010.

[5] A. Alabdulwahab, A. Abusorrah, X. Zhang, and M. Shahidehpour, "Coordination of Interdependent Natural Gas and Electricity Infrastructures for Firming the Variability of Wind Energy in Stochastic Day-Ahead Scheduling," *Sustainable Energy, IEEE Transactions on,* vol. 6, pp. 606-615, 2015.

[6] T. Li, M. Eremia, and M. Shahidehpour, "Interdependency of Natural Gas Network and Power System Security," *IEEE Transactions on Power Systems,* vol. 23, pp. 1817-1824, Nov 2008.

[7] C. M. Correa-Posada and P. Sanchez-Martin, "Integrated Power and Natural Gas Model for Energy Adequacy in Short-Term Operation," *Power Systems, IEEE Transactions on,* vol. 30, pp. 3347-3355, 2015.

[8] P. Duenas, T. Leung, M. Gil, and J. Reneses, "Gas-Electricity Coordination in Competitive Markets Under Renewable Energy Uncertainty," *Power Systems, IEEE Transactions on,* vol. 30, pp. 123-131, 2015.

[9] M. Shahidehpour, Y. Fu, and T. Wiedman, "Impact of natural gas infrastructure on electric power systems," *Proceedings of the IEEE,* vol. 93, pp. 1042-1056, May 2005.

[10] C. Liu, M. Shahidehpour, and J. Wang, "Coordinated scheduling of electricity and natural gas infrastructures with a transient model for natural gas flow," *Chaos,* vol. 21, p. 025102, 2011.

[11] A. Thorley and C. Tiley, "Unsteady and transient flow of compressible fluids in pipelines—a review of theoretical and some experimental studies," *International Journal of Heat and Fluid Flow,* vol. 8, pp. 3-15, 1987.

[12] A. D. Woldeyohannes and M. A. A. Majid, "Simulation model for natural gas transmission pipeline network system," *Simulation Modelling Practice and Theory,* vol. 19, pp. 196-212, 2011.

[13] M. Behbahani-Nejad and A. Bagheri, "The accuracy and efficiency of a MATLAB-Simulink library for transient flow simulation of gas pipelines and networks," *Journal of Petroleum Science and Engineering,* vol. 70, pp. 256-265, 2// 2010.

[14] T. Kiuchi, "An implicit method for transient gas flows in pipe networks," *International Journal of Heat and Fluid Flow,* vol. 15, pp. 378-383, 1994.

[15] E. B. Wylie, M. A. Stoner, and V. L. Streeter, "Network: System transient calculations by implicit method," *Society of Petroleum Engineers Journal,* vol. 11, pp. 356-362, 1971.

[16] A. Zlotnik, M. Chertkov, and S. Backhaus, "Optimal control of transient flow in natural gas networks," *arXiv preprint arXiv:1504.02505,* 2015.

[17] S. Grundel, N. Hornung, B. Klaassen, P. Benner, and T. Clees, "Computing surrogates for gas network simulation using model order

reduction," in *Surrogate-Based Modeling and Optimization*, ed: Springer, 2013, pp. 189-212.

[18] M. Chertkov, M. Fisher, S. Backhaus, R. Bent, and S. Misra, "Pressure Fluctuations in Natural Gas Networks caused by Gas-Electric Coupling," *2015 48th Hawaii International Conference on System Sciences (Hicss),* pp. 2738-2747, 2015.

[19] X. Xu, H. J. Jia, H. D. Chiang, D. C. Yu, and D. Wang, "Dynamic Modeling and Interaction of Hybrid Natural Gas and Electricity Supply System in Microgrid," *IEEE Transactions on Power Systems,* vol. 30, pp. 1212-1221, May 2015.

[20] A. Abdul-Ameer, "The Modelling and Simulation of Gas Pipeline Dynamic," presented at the Recent Researches in Automatic Control, Systems Science and Communications, Porto, 2012.

[21] R. Whalley and A. A-Ameer, "The computation of torsional, dynamic stresses," *Proceedings of the Institution of Mechanical Engineers, Part C: Journal of Mechanical Engineering Science,* vol. 223, pp. 1799-1814, August 1, 2009 2009.

[22] J. F. Helgaker, B. Muller, and T. Ytrehus, "Transient Flow in Natural Gas Pipelines Using Implicit Finite Difference Schemes," *Journal of Offshore Mechanics and Arctic Engineering-Transactions of the Asme,* vol. 136, Aug 2014.

[23] D. V. Widder, *Laplace Transform (PMS-6)*: Princeton University Press, 2015.

[24] S. Skogestad, "Simple analytic rules for model reduction and PID controller tuning," *Journal of Process Control,* vol. 13, pp. 291-309, 2003.

[25] U. S. EIA. (2016, March 20). *SAS Output.* Available: https://www.eia.gov/electricity/annual/html/epa_08_02.html

[26] E. B. Wylie, V. L. Streeter, and M. A. Stoner, "Network System Transient Calculations by Implicit Method," *Society of Petroleum Engineers Journal,* vol. 11, pp. 356-&, 1971.

[27] C. f. T. Analysis. (2016). *Lower and Higher Heating Values of Gas, Liquid and Solid Fuels.* Available: http://cta.ornl.gov/bedb/appendix_a/Lower_and_Higher_Heating_Values_of_Gas_Liquid_and_Solid_Fuels.pdf

Yongzhi Zhou received the B.S. degree in College of Electrical Engineering, Shandong University, China, in 2008. He then worked as an operator at a thermal power plant from 2008 to 2012. He is a Ph. D. candidate in College of Electrical Engineering, Zhejiang University since 2012. He was visiting the University of Bath from September 2015 to March 2016.

Chenghong Gu (M'14) was born in Anhui province, China. He obtained Bachelor degree and Master degree in electrical engineering from Shanghai University of Electric Power and Shanghai Jiao Tong University in China in 2003 and 2007 respectively. In 2010, he obtained his Ph.D. from University of Bath, U.K. Now, he is a Lecturer and EPSRC fellow with the Dept. of Electronic & Electrical Eng., University of Bath, UK. His major research is in multi-vector energy system, smart grid and power economics.

Hao Wu (M10) received the B.A. degree from Shanghai Jiao Tong University, Shanghai, China, and the Ph.D. degree from Zhejiang University, Hangzhou, Zhejiang, China, both in electrical engineering. He was with Zhejiang University since 2002 and currently he is an Associate Professor.

Yonghua Song (F'08) is Executive Vice-President of Zhejiang University. He is a fellow of the Royal Academy of Engineering, a fellow of the IEEE and Vice- President of Chinese Society for Electrical Engineering (CSEE). He received his BEng and PhD from Chengdu University of Science and Technology, and China Electric Power Research Institute in 1984 and 1989 respectively. In January 2007, he took up a Pro-Vice Chancellorship and Professorship of Electrical Engineering at the University of Liverpool.